SPACE-TIME CODING FOR DOUBLY-SELECTIVE CHANNELS*

Xiaoli Ma and *Georgios B. Giannakis*
Dept. of ECE, University of Minnesota, Minneapolis, MN 55455, USA

ABSTRACT

Relying on a basis expansion model (BEM) to capture time- and frequency-selective propagation effects, we prove that the maximum achievable diversity of multi-antenna transmissions over doubly-selective channels is determined by the rank of the correlation matrix of the BEM coefficients from all channels. The diversity order is multiplicative in the effective degrees of freedom that the channels exhibit in space-, time-, and frequency-domains. Furthermore, we design a block precoded digital phase sweeping transmission that achieves full space-Doppler-multipath diversity for any number of transmit-receive antennas, and without bandwidth expansion. The theoretical diversity results are corroborated by simulations, and the BEM is validated.

1. INTRODUCTION

Multipath propagation through wireless channels introduces frequency selectivity which increases along with the demand for higher data rates. Furthermore, temporal channel variations arising due to relative mobility between transmitter and receiver, as well as due to oscillator drifts and phase noise, give rise to time-selectivity. The combined time-frequency selectivity induces Doppler-multipath fading, which affects critically communication performance. This motivates research towards efficient coding and modulation schemes that improve the quality of rapidly fading wireless links.

Naturally, the Doppler diversity is induced by time-selective channel effects [1, 4, 5]. But one can also inject it intentionally to enhance diversity, or even introduce it, by a so-termed phase sweeping transmission that "creates time-variations" of an originally slow-fading channel [2, 3]. Because doubly-selective channels entail more degrees of freedom than time-selective ones, they offer the potential for higher diversity gains [4, 5]. Unfortunately, the phase-sweeping-based approaches of [2, 3] are bandwidth consuming, and they are not designed to bring joint Doppler-multipath benefits. Furthermore, boosting the diversity of doubly-selective channels by deploying multiple antennas has not been discussed in [2, 3, 4, 5]. An attempt to collect both space and Doppler diversity gains was made in [7], through the design of the so-called "smart-greedy" codes. However, these codes are not tailored to specifically exploit the underlying channel variations.

In this paper, doubly-selective channel effects are modeled by a Basis Expansion Model (BEM) (see [1, 4] and references therein), which allows one to quantify the maximum diversity order. Using this BEM, we then develop a block precoded *digital* phase sweeping scheme that achieves the maximum possible space-Doppler-multipath diversity gain for any number of transmit-receive antennas, and without bandwidth expansion.

Notation: Upper (lower) bold face letters will be used for matrices (column vectors). Superscript $^{\mathcal{H}}$ will denote Hermitian, * conjugate, ^{T} transpose, and $\dagger$ pseudo-inverse. We will reserve E[$\cdot$] for expectation. We will use $[\mathbf{A}]_{k,m}$ to denote the (k, m)th entry of a matrix $\mathbf{A}$, and $[\mathbf{x}]_m$ to denote the mth entry of the column vector $\mathbf{x}$. $\mathbf{I}_N$ will denote the $N \times N$ identity matrix, and $\mathbf{F}_N$ the $N \times N$ normalized FFT matrix; diag[$\mathbf{x}$] will stand for a diagonal matrix with $\mathbf{x}$ on its main diagonal; $N_t (N_r)$ will be the number of transmit (receive) antennas, and T_s will stand for the sampling period.

*The work in this paper was supported by the NSF Wireless Initiative Grant No. 9979443, NSF Grant No. 0122431, and by the ARL/CTA Grant No. DAAD19-01-2-011.

2. BLOCK TRANSMISSION SYSTEM MODEL

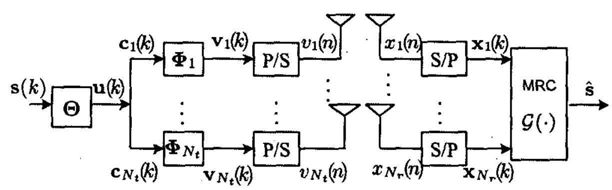

Fig. 1. Discrete-time model of transmitter and receiver.

The information bearing symbols $s(n)$ are drawn from a finite alphabet, and parsed into blocks of size $M \times 1$: $[\mathbf{s}(k)]_m := s(kM + m)$. Each block $\mathbf{s}(k)$ is linearly precoded by the $N \times M$ matrix $\boldsymbol{\Theta}$, resulting into $\mathbf{u}(k) := \boldsymbol{\Theta}\mathbf{s}(k)$. Each block $\mathbf{u}(k)$ is further transformed into N_t blocks $\{\mathbf{c}_\mu(k)\}_{\mu=1}^{N_t}$ of size $N \times 1$. Each block $\mathbf{c}_\mu(k)$ is finally linearly processed by the $N \times N$ matrix $\boldsymbol{\Phi}_\mu$, resulting into $\mathbf{v}_\mu(k) := \boldsymbol{\Phi}_\mu \mathbf{c}_\mu(k)$. The sequence $v_\mu(n)$ obtained by serial-to-parallel converting $\mathbf{v}_\mu(k)$ is then pulse-shaped, carrier modulated, and transmitted from the μth transmit-antenna. The nth sample at the νth receive-antenna is given by:

$$x_\nu(n) = \sum_{\mu=1}^{N_t} \sum_{l=0}^{L} h^{(\nu,\mu)}(n; l) v_\mu(n - l) + \zeta_\nu(n), \qquad (1)$$

where $\{h^{(\nu,\mu)}(n; l)\}_{l=0}^{L}$ is the Lth order doubly-selective channel response from the μth transmit-antenna to the νth receive-antenna (notice the channel dependence on n), and $\zeta_\nu(n)$ is complex additive white Gaussian noise (AWGN) at the νth receive-antenna with mean zero and variance $N_0/2$. As in [4], we model the channel $\forall \nu \in [1, N_r]$, $\mu \in [1, N_t]$, using a Fourier basis expansion:

$$h^{(\nu,\mu)}(n; l) := \sum_{q=0}^{Q} h_q^{(\nu,\mu)}(\lfloor \frac{n}{N} \rfloor; l) e^{j\omega_q (n \bmod N)}, \forall l \in [0, L], \qquad (2)$$

where $\omega_q := 2\pi(q - Q/2)/N$, $Q := 2\lceil f_{\max} N T_s \rceil$, and $L := \lfloor \tau_{\max}/T_s \rfloor$, with the parameters $f_{\max}$ and $\tau_{\max}$ denoting the channel's Doppler spread and delay spread, respectively. Because they can be measured experimentally in practice, we assume that $f_{\max}$ and $\tau_{\max}$ (and thus Q and L) are known.

At each receive-antenna, the symbol rate sampled sequence $x_\nu(n)$ at the receive-filter output is serial-to-parallel converted to form the $N \times 1$ blocks $[\mathbf{x}_\nu(k)]_n := x_\nu(kN+n)$. Suppose the transmitter has been designed to remove the inter-block interference. Later, we will see that our design satisfies this condition. The matrix-vector counterpart of (1) can then be expressed as:

$$\mathbf{x}_\nu(k) = \sum_{\mu=1}^{N_t} \mathbf{H}^{(\nu,\mu)}(k)\mathbf{v}_\mu(k) + \boldsymbol{\zeta}_\nu(k), \quad \forall \nu \in [1, N_r], \quad (3)$$

where

$$\mathbf{H}^{(\nu,\mu)}(k) := \sum_{q=0}^{Q} \mathbf{D}_q \mathbf{H}_q^{(\nu,\mu)}(k) \quad (4)$$

is an $N \times N$ diagonal matrix, with $\mathbf{D}_q := \text{diag}[1, \exp(j\omega_q), \ldots, \exp(j\omega_q(N-1))]$, and $\mathbf{H}_q^{(\nu,\mu)}$ is a lower triangular Toeplitz matrix with first column $[h_q^{(\nu,\mu)}(0), \ldots, h_q^{(\nu,\mu)}(L), 0, \ldots, 0]^T$. Each block $\mathbf{x}_\nu(k)$ is finally decoded by $\mathcal{G}(\cdot)$ to obtain an estimate of $\mathbf{s}(k)$ as: $\hat{\mathbf{s}}(k) := \mathcal{G}(\{\mathbf{x}_\nu(k)\}_{\nu=1}^{N_r})$.

In this paper, we will show how to design the ST encoder and decoder in order to collect joint space-multipath-Doppler diversity. Since in the following we will work on a block-by-block basis, we will drop the block index k.

3. DESIGN AND PERFORMANCE CRITERIA

In this section, we will design criteria for our ST coding. Our derivations are based on the following operating conditions:

A1) Channel coefficients $h_q^{(\nu,\mu)}(l)$ are zero mean, possibly correlated, complex Gaussian random variables;

A2) Channel state information (CSI) is perfectly known at the receiver, but unknown at the transmitter;

A3) High SNR is considered for deriving the diversity order;

A4) Channels $\mathbf{H}^{(\nu,\mu)}$ in (4) satisfy: $\det\left[\sum_{\nu=1}^{N_r}\left(\sum_{\mu=1}^{N_t}\mathbf{H}^{(\nu,\mu)}(k)\right)\left(\sum_{\mu=1}^{N_t}(\mathbf{H}^{(\nu,\mu)}(k))^{\mathcal{H}}\right)\right] \neq 0$.

When transmissions experience rich scattering and no line-of-sight is present, the central limit theorem validates A1). A4) is more technical rather than restrictive, since it guarantees that not all channels are identically zero at the same time slot. For random channels, A4) excludes an event with probability zero. The usefulness of A4) per channel realization, is to ensure invertibility of the matrix which is required for decoding and performance analysis.

We consider here the best performance possible with ST coded transmissions. Similar to [7], we will resort to pairwise error probability (PEP) analysis to design our optimality criteria. Define the PEP, $P(\mathbf{s} \to \mathbf{s}'|\mathbf{H}^{(\nu,\mu)}, \forall \nu, \mu)$, as the probability that maximum likelihood (ML) decoding of $\mathbf{s}$ erroneously decides $\mathbf{s}'$ in favor of the actually transmitted $\mathbf{v}$.

According to (3), ML decoding of $\mathbf{v}$ amounts to:

$$\hat{\mathbf{s}} = \arg\min_{\bar{\mathbf{v}}_\mu \in \mathcal{A}_v^\mu} \sum_{\nu=1}^{N_r} \left\| \mathbf{x}_\nu - \sum_{\mu=1}^{N_t} \mathbf{H}^{(\nu,\mu)}\bar{\mathbf{v}}_\mu \right\|^2, \quad (5)$$

where $\bar{\mathbf{v}}_\mu$ is the candidate $\mathbf{v}_\mu$, $\mathcal{A}_v^\mu$ is the finite alphabet for $\mathbf{v}_\mu$, and $\|\cdot\|$ denotes the Frobenius norm. Conditioned on $\mathbf{H}^{(\nu,\mu)}$'s, the Chernoff bound on the PEP yields [7]:

$$P(\mathbf{s} \to \mathbf{s}'|\mathbf{H}^{(\nu,\mu)}, \forall \nu, \mu) \leq \exp\left(-\frac{d^2(\tilde{\mathbf{x}}, \tilde{\mathbf{x}}')}{4N_0}\right), \quad (6)$$

where $\tilde{\mathbf{x}} := [(\sum_{\mu=1}^{N_t} \mathbf{H}^{(1,\mu)}\mathbf{v}_\mu)^T, \ldots, (\sum_{\mu=1}^{N_t} \mathbf{H}^{(N_r,\mu)}\mathbf{v}_\mu)^T]^T$; while the distance in the exponent is

$$d^2(\tilde{\mathbf{x}}, \tilde{\mathbf{x}}') = \sum_{\nu=1}^{N_r} \left\| \sum_{\mu=1}^{N_t} \sum_{q=0}^{Q} \mathbf{D}_q \mathbf{E}_\mu \mathbf{h}_q^{(\nu,\mu)} \right\|^2,$$

and $\mathbf{E}_\mu$ is an $N \times (Q+1)$ Toeplitz matrix with first column $[\mathbf{e}_\mu^T, 0 \ldots, 0]^T$, $\mathbf{e}_\mu := \mathbf{v}_\mu - \mathbf{v}'_\mu$, and $\mathbf{h}_q^{(\nu,\mu)} := [h_q^{(\nu,\mu)}(0), \ldots, h_q^{(\nu,\mu)}(L)]^T$. With these definitions, we can rewrite $d^2(\tilde{\mathbf{x}}, \tilde{\mathbf{x}}')$ as:

$$d^2(\tilde{\mathbf{x}}, \tilde{\mathbf{x}}') = \mathbf{h}^{\mathcal{H}}\mathbf{A}_e\mathbf{h},$$

where

$$\begin{aligned} \mathbf{h} &:= [\mathbf{h}^{(1,1)}, \ldots, \mathbf{h}^{(1,N_t)}, \ldots, \mathbf{h}^{(N_r,N_t)}]^T, \\ \mathbf{h}^{(\nu,\mu)} &:= [h_0^{(\nu,\mu)}(0), \ldots, h_0^{(\nu,\mu)}(L), \ldots, h_Q^{(\nu,\mu)}(L)], \\ \mathbf{A}_e &:= \mathbf{I}_{N_r} \otimes (\mathbf{\Phi}_e^{\mathcal{H}}\mathbf{\Phi}_e), \\ \mathbf{\Phi}_e &:= [\mathbf{\Omega}_e^{(1)}, \ldots, \mathbf{\Omega}_e^{(N_t)}], \\ \mathbf{\Omega}_e^{(\mu)} &:= [\mathbf{D}_0\mathbf{E}_\mu, \ldots, \mathbf{D}_Q\mathbf{E}_\mu], \end{aligned} \quad (7)$$

with $\otimes$ denoting the Kronecker product. Since our analysis will allow for correlated channels, we will denote the channel correlation matrix and its rank, respectively, by:

$$\begin{aligned} \mathbf{R}_h &:= \text{E}[\mathbf{h}\mathbf{h}^{\mathcal{H}}], \\ \text{and } r_h &:= \text{rank}(\mathbf{R}_h) \leq N_t N_r (L+1)(Q+1). \end{aligned} \quad (8)$$

Eigenvalue decomposition of $\mathbf{R}_h$ yields $\mathbf{R}_h = \mathbf{U}_h\mathbf{\Lambda}_h\mathbf{U}_h^{\mathcal{H}}$, where $\mathbf{\Lambda}_h := \text{diag}[\sigma_0^2, \ldots, \sigma_{r_h-1}^2]$, and $\mathbf{U}_h$ is an $N_t N_r(L+1)(Q+1) \times r_h$ para-unitary matrix satisfying $\mathbf{U}_h^{\mathcal{H}}\mathbf{U}_h = \mathbf{I}_{r_h}$. Define an $r_h \times 1$ normalized channel vector $\bar{\mathbf{h}}$ with entries $\bar{h}_q^{(\nu,\mu)}$ that are i.i.d. Gaussian distributed, with zero mean and unit variance. It is easy to show that $\mathbf{h}$ and $\mathbf{U}_h\mathbf{\Lambda}_h^{1/2}\bar{\mathbf{h}}$ have identical distributions. Therefore, the PEP remains statistically invariant when we plug in $\mathbf{U}_h\mathbf{\Lambda}_h^{1/2}\bar{\mathbf{h}}$ instead of $\mathbf{h}$. To proceed, let us define

$$\mathbf{\Psi}_e := (\mathbf{U}_h\mathbf{\Lambda}_h^{1/2})^{\mathcal{H}}\mathbf{A}_e\mathbf{U}_h\mathbf{\Lambda}_h^{1/2}. \quad (9)$$

Since $\mathbf{\Psi}_e$ is Hermitian, there exists a unitary matrix $\mathbf{U}_e$, and a real non-negative definite diagonal matrix $\mathbf{\Lambda}_e$ so that $\mathbf{U}_e^{\mathcal{H}}\mathbf{\Psi}_e\mathbf{U}_e = \mathbf{\Lambda}_e$. The $r_h \times r_h$ diagonal matrix $\mathbf{\Lambda}_e := \text{diag}[\lambda_0, \ldots, \lambda_{r_h-1}]$, holds on its diagonal the eigenvalues of $\mathbf{\Psi}_e$, that satisfy $\lambda_m \geq 0$, $\forall m \in [0, r_h-1]$. The vector $\tilde{\mathbf{h}} = \mathbf{U}_e\bar{\mathbf{h}}$ has the same distribution as $\bar{\mathbf{h}}$, because $\mathbf{U}_e$ is unitary. Thus, $d^2(\tilde{\mathbf{x}}, \tilde{\mathbf{x}}')$ can be rewritten in terms of the eigenvalues of the matrix $\mathbf{\Psi}_e$ as

$$d^2(\tilde{\mathbf{x}}, \tilde{\mathbf{x}}') = \sum_{m=0}^{r_h-1} \lambda_m |\tilde{h}_m|^2. \quad (10)$$

Since we wish our ST coders to be independent of the particular channel realization, it is appropriate to average the PEP over the independent Rayleigh distributed $|\tilde{h}_m|^2$'s. If $r_e := \text{rank}(\mathbf{\Psi}_e)$, then r_e eigenvalues of $\mathbf{\Psi}_e$ are non-zero; without loss of generality, we denote these eigenvalues as $\lambda_0 \geq \cdots \geq \lambda_{r_e-1}$. At high SNR, the resulting average PEP is bounded as follows:

$$\bar{P}(\mathbf{s} \to \mathbf{s}') \leq \prod_{m=0}^{r_e-1} \left(\frac{\lambda_m}{4N_0}\right)^{-1} = \left(G_{e,c}\frac{1}{4N_0}\right)^{-G_{e,d}}, \quad (11)$$

where $G_{e,d} := r_e$ is the diversity order, and $G_{e,c} := \left(\prod_{m=0}^{r_e-1}\lambda_m\right)^{\frac{1}{r_e}}$ is the coding gain for the error pattern $\mathbf{e} := \mathbf{s} - \mathbf{s}'$. Accounting for all possible pairwise errors, we define herein the diversity and coding gains for our multi-antenna systems, respectively, as:

$$G_d := \min_{\forall \mathbf{e} \neq 0} G_{e,d}, \quad \text{and} \quad G_c := \min_{\forall \mathbf{e} \neq 0} G_{e,c}. \quad (12)$$

Because the performance of ST depends on both G_d and G_c, it is important to maximize both of them. Before specializing to particular ST designs, we wish to quantify the maximum possible G_d and G_c.

Eq. (11) discloses that G_d depends on the rank of Ψ_e. By checking the dimensionality of Ψ_e, we recognize that by appropriately designing our transmission, it is possible to achieve a maximum (and thus optimum) diversity order

$$G_d^{\max} = r_h \leq N_t N_r (L+1)(Q+1), \tag{13}$$

if and only if the matrix Ψ_e has full rank r_h, $\forall \mathbf{e} \neq \mathbf{0}$.

In summary, we have established the following proposition:

Proposition 1: *Consider (N_t, N_r) multi-antenna transmissions through doubly-selective channels adhering to a BEM with $Q+1$ bases and $L+1$ taps. If the correlation matrix of the channel coefficients in (8) has rank r_h, then the maximum diversity order of transmissions in (3) is $G_d = r_h$.*

4. DIGITAL PHASE SWEEPING

The phase sweeping method can be viewed as the dual of delay-diversity, which was originally developed for converting ST frequency-flat channels into a single frequency-selective channel [6]. But one can also think of converting ST frequency-selective channels into a single but longer frequency-selective channel. We will show that Digital Phase Sweeping (DPS) can also convert ST time-selective channels into a single faster time-selective channel. The analog phase sweeping (a.k.a. intentional frequency offset) idea was introduced in [2]. Later on, [3] combined the phase sweeping idea with channel coding to further improve the performance. However, the designs in [2] and [3] are analog, and as such they incur bandwidth expansion. Without an explicit channel model, they are unable to quantify the diversity gain. Here, we will design a DPS for doubly-selective channels that does not expand bandwidth, and is capable of quantifying and collecting the full diversity gain for any number of transmit-receive antennas.

4.1. Encoding of DPS

By equally allocating the transmit-power, we set $\mathbf{c}_\mu = \mathbf{u}/\sqrt{N_t}$, $\forall \mu \in [1, N_t]$. Using (3), $\mathbf{x}_\nu$ and $\mathbf{s}$ can then be related via:

$$\mathbf{x}_\nu = \frac{1}{\sqrt{N_t}} \sum_{\mu=1}^{N_t} \mathbf{H}^{(\nu,\mu)} \mathbf{\Phi}_\mu \mathbf{\Theta} \mathbf{s} + \boldsymbol{\zeta}_\nu, \ \ \forall \nu \in [1, N_r]. \tag{14}$$

Observing (4), we notice that different channels share the same exponential bases, but have different channel coefficients. Our idea is to shift the $Q+1$ bases of each channel corresponding to one of the N_t transmit antennas so that all the bases become consecutive on the FFT grid of complex exponentials. This will render the N_t channels to each receive-antenna equivalent to a single doubly-selective channel with $N_t(Q+1)$ bases. Mathematically, the matrices $\{\mathbf{\Phi}_\mu\}_{\mu=1}^{N_t}$, that implement DPS, are designed as

$$\mathbf{\Phi}_\mu := \text{diag}[1, e^{j\phi_\mu}, \ldots, e^{j\phi_\mu(N-1)}], \ \ \forall \mu \in [1, N_t], \tag{15}$$

where $\phi_\mu := 2\pi(\mu-1)(Q+1)/N$. Recalling the structure of $\mathbf{H}_q^{(\nu,\mu)}$ in (4), we have

$$\mathbf{H}_q^{(\nu,\mu)} \mathbf{\Phi}_\mu = \mathbf{\Phi}_\mu \bar{\mathbf{H}}_q^{(\nu,\mu)}, \ \ \forall q, \nu, \mu, \tag{16}$$

where $\bar{\mathbf{H}}_q^{(\nu,\mu)}$ has the same structure as $\mathbf{H}_q^{(\nu,\mu)}$, but the first column is $[h_q(0), h_q(1)e^{j\omega_q}, \ldots, h_q(L)e^{j\omega_q L}, 0, \ldots, 0]^T$. Considering the designs in (15), Eq. (14) can be rewritten as

$$\mathbf{x}_\nu = \frac{1}{\sqrt{N_t}} \sum_{q=0}^{N_t(Q+1)-1} \mathbf{D}_q \mathbf{H}_q^{(\nu)} \mathbf{\Theta} \mathbf{s} + \boldsymbol{\zeta}_\nu, \ \ \forall \nu \in [1, N_r], \tag{17}$$

where $\mathbf{H}_q^{(\nu)} := \bar{\mathbf{H}}_{\text{mod}(q,Q+1)}^{(\nu, \lfloor q/(Q+1) \rfloor + 1)}$.

Comparing (17) with the model of [4], we observe that this DPS design transforms the N_t transmit-antenna scenario, where each channel can be expressed via $Q+1$ exponential bases, into a single transmit-antenna scenario, where the equivalent channel can be expressed by $N_t(Q+1)$ Fourier bases. Hence, relying on the precoder $\mathbf{\Theta}$ and $\mathcal{G}(\cdot)$, we can now apply any single-input multi (single)-output method for doubly-selective channels to ensure the maximum diversity gain. Here, we adopt the time-frequency precoder with time-frequency guards [4]:

$$\mathbf{\Theta} = (\mathbf{F}_{P+N_t(Q+1)-1}^{\mathcal{H}} \mathbf{T}_f) \otimes \mathbf{T}_t, \tag{18}$$

where $\mathbf{T}_f := [\mathbf{I}_P, \mathbf{0}_{P \times (Nt(Q+1)-1)}]^T$ places the frequency guard, and $\mathbf{T}_t := [\mathbf{I}_K, \mathbf{0}_{K \times L}]^T$ inserts the time guard. We define $M = PK$, and $N = (P + N_t(Q+1) - 1)(K+L)$. The precoder in (18) enables the full multipath-Doppler diversity (see [4] for detailed proofs).

4.2. Decoding of DPS

For convenience, we define

$$\mathbf{H}^{(\nu)} = \textstyle\sum_{q=0}^{N_t(Q+1)-1} \mathbf{D}_q \mathbf{H}_q^{(\nu)}, \ \ \forall \nu \in [1, N_r]. \tag{19}$$

Since the received blocks $\mathbf{y}_\nu$ from all N_r receive-antennas contain the information block $\mathbf{s}$, we combine the information from all received blocks when decoding $\mathbf{s}$. To retain decoding optimality, we select the maximum ratio combining (MRC) method. The MRC for $\mathbf{x}_\nu$ in (17), amounts to multi-channel filtering with the matrix

$$\mathbf{G} = \left(\sum_{\nu=1}^{N_r} \left(\mathbf{H}^{(\nu)}\right)^{\mathcal{H}} \mathbf{H}^{(\nu)} \right)^{-\frac{1}{2}} \left[(\mathbf{H}^{(1)})^{\mathcal{H}}, \ldots, (\mathbf{H}^{(N_r)})^{\mathcal{H}} \right]. \tag{20}$$

The MRC output $\mathbf{y}$, is then given by:

$$\mathbf{y} = \mathbf{G} \begin{bmatrix} \mathbf{x}_1 \\ \vdots \\ \mathbf{x}_{N_r} \end{bmatrix} = \frac{1}{\sqrt{N_t}} \left(\sum_{\nu=1}^{N_r} \left(\mathbf{H}^{(\nu)}\right)^{\mathcal{H}} \mathbf{H}^{(\nu)} \right)^{\frac{1}{2}} \mathbf{\Theta} \mathbf{s} + \boldsymbol{\eta}, \tag{21}$$

where $\boldsymbol{\eta} := \mathbf{G}[\boldsymbol{\zeta}_1^T, \ldots, \boldsymbol{\zeta}_{N_r}^T]^T$. Thanks to A5), it can be verified that $\mathbf{G}$ is para-unitary; i.e., $\mathbf{G}\mathbf{G}^{\mathcal{H}} = \mathbf{I}$. Since $\boldsymbol{\zeta}_\nu$'s are independent AWGN vectors, the noise vector $\boldsymbol{\eta}$ is still white. ML decoding achieves the full diversity r_h, if the linear precoder $\mathbf{\Theta}$ is designed according to [4]. Based on the PEP analysis in Section 3, we have proved that the maximum space-multipath-Doppler diversity is guaranteed by our linearly precoded DPS design. Due to space limitation, we omit the proof here, and summarize our result in the following proposition:

Proposition 2: *The achievable full diversity order $G_d^{\max} = r_h$ for multi-antenna transmissions over doubly-selective channels is guaranteed by our DPS design.*

ML decoding achieves full diversity. However, as the number of antennas increases, the block length increases as well. ML decoding for the entire $N \times 1$ block entails high computational complexity. To reduce the decoding complexity, we can use suboptimum linear equalization. By defining

$$\mathbf{H}_{eq} := \tfrac{1}{\sqrt{N_t}} \left(\textstyle\sum_{\nu=1}^{N_r} \left(\mathbf{H}^{(\nu)}\right)^{\mathcal{H}} \mathbf{H}^{(\nu)} \right)^{\frac{1}{2}} \mathbf{\Theta}, \tag{22}$$

we express the ZF and the MMSE equalizers, respectively, as

$$\mathbf{G}_{zf} = \mathbf{H}_{eq}^{\dagger}, \ \text{ and}$$

$$\mathbf{G}_{mmse} = \mathbf{R}_{ss} \mathbf{H}_{eq}^{\mathcal{H}} (\sigma_\eta^2 \mathbf{I}_{N_s} + \mathbf{H}_{eq} \mathbf{R}_{ss} \mathbf{H}_{eq}^{\mathcal{H}})^{-1}, \tag{23}$$

where $\mathbf{R}_{ss} := \mathrm{E}[\mathbf{s}\mathbf{s}^{\mathcal{H}}]$ is the autocorrelation matrix of $\mathbf{s}$. It is well-known that linear equalizers have lower computational complexity than ML decoders. However, they are unable to collect the full diversity order offered by our transmissions.

In a nutshell, the matrices $\{\mathbf{\Phi}_\mu\}_{\mu=1}^{N_t}$ in (14) induce digital phase sweeping to our block transmissions, reminiscent of that used in [2, 3], to increase the variation (and thus the diversity gain) of time-varying channels. The differences between our design and [2, 3] are: i) our design subsumes schemes for time- or frequency-selective channels; ii) we collect not only space-diversity as in [2, 3], but also Doppler-multipath diversity; iii) we generalize the phase sweeping idea to multiple transmit- and receive-antennas; iv) DPS can be used not only for coded, but also for uncoded systems; v) compared with the analog designs in [2, 3], our digital design does not expand bandwidth.

Remark: The ability of DPS to convert multi-antenna ST transmissions to single-antenna transmissions over doubly selective channels, facilitates also optimal training for channel estimation; hence, existing SISO training algorithms can be applied directly to our ST-MIMO system with DPS.

5. SIMULATED PERFORMANCE

We now present simulations to test the BEM fitting to doubly-selective channels, and also confirm the performance of our multi-antenna ST transmissions over time-varying channels.

Test Case 1: (Time-selective channels) The purpose of this example is two-fold: to validate our BEM by comparing it with the Jakes' model; and also to verify our DPS design on time-selective channels which are special cases of doubly-selective channels. We consider a carrier frequency $f_0 = 900$ MHz, and a mobile speed $v_{\max} = 96$ km/hr. The transmitted block length is $N = 25$. Since we want to test the diversity for different Q's, we select the symbol period $T_s = Q/(2f_{\max}N)$. We generate all multiple channels using this Jakes' model. At the transmitter, we adopt our DPS design with $\Theta = \mathbf{F}^{\mathcal{H}}\mathbf{T}_f$ as in (18). At the receiver, we consider MMSE equalization for two different scenarios: one uses the parameters generated by the Jakes' model (corresponding curves are marked by "Jakes" in Fig. 2); and the other one uses the BEM coefficients that approximate the Jakes' model (see [4] for details). Fig. 2 depicts the performance results. We observe that: i) our DPS design enables spatial diversity gains even for channels adhering to the Jakes' model; ii) when Q is small (e.g., $Q = 2$), model mismatch between the BEM and the Jakes' model causes an error floor; and iii) when Q is large, the BEM matches the Jakes' model well, and the BER performance improves considerably.

Test Case 2: (Doubly-selective channels) In this example, we will test our claims of Section 4 for multiplicative diversity gain with BPSK transmissions. We select the number of antennas as $(N_t, N_r) = (2, 1)$ and Θ as in (18). The channel coefficients are generated as i.i.d. zero-mean Gaussian random variables with variance $1/((L+1)(Q+1))$. Fig. 3 depicts the performance of ZF equalization, along with the near-ML equalizer implemented with the Sphere-Decoding (SD) algorithm. We notice that as Q or L increases, the performance (diversity order) increases. SD outperforms ZF equalization only by about 1dB when BER= 10^{-3}, and $(Q, L) = (2, 2)$. Hence, we observe that when the channels' potential diversity order is high, the linear equalizers can afford acceptable BER performance with reduced complexity.

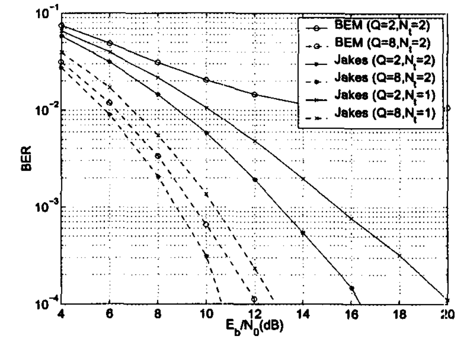

Fig. 2. Validation of the BEM based on Jakes' model

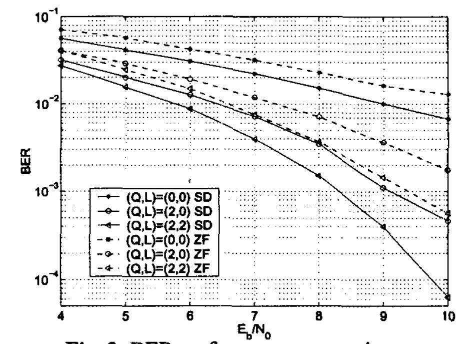

Fig. 3. BER performance comparisons

6. REFERENCES

[1] G. B. Giannakis and C. Tepedelenlioğlu, "Basis Expansion Models and Diversity Techniques for Blind Identification and Equalization of Time-Varying Channels," *Proceedings of the IEEE*, pp. 1969-1986, Nov. 1998.

[2] A. Hiroike, F. Adachi, and N. Nakajima, "Combined Effects of Phase Sweeping Transmitter Diversity and Channel Coding," *IEEE Trans. on Vehic. Techn.*, pp. 170–176, May 1992.

[3] W.-Y. Kuo and M. P. Fitz, "Design and Analysis of Transmitter Diversity Using Intentional Frequency Offset for Wireless Communications," *IEEE Trans. on Vehicular Technology*, vol. 46, no. 4, pp. 871–881, Nov. 1997.

[4] X. Ma, and G. B. Giannakis, "Designing Maximum Multipath-Doppler Diversity Transmissions over Time- and Frequency-Selective Wireless Channels," *Proc. of 39th Allerton Conf.*, Monticello, IL, Oct. 3-5, 2001.

[5] A. M. Sayeed and B. Aazhang, "Joint Multipath-Doppler Diversity in Mobile Wireless Communications," *IEEE Trans. on Communications*, vol. 47, no.1, pp. 123–132, Jan. 1999.

[6] N. Seshadri, and J. H. Winters, "Two Signaling Schemes for Improving the Error Performance of Frequency-Division Duplex (FDD) Transmission Systems using Transmitter Antenna Diversity," *Intl. Journal of Wireless Info. Networks*, pp. 49–60, 1994.

[7] V. Tarokh, N. Seshadri, and A. R. Calderbank, "Space-Time Codes for High Data Rate Wireless Communication: Performance Criterion and Code Construction," *IEEE Trans. on Information Theory*, pp. 744–765, Mar. 1998.